Monthly Notices of the ROYAL ASTRONOMICAL SOCIETY

MNRAS **533,** 2916–2926 (2024) https://doi.org/10.1093/mnras/stae1958
Advance Access publication 2024 August 14

Most frequent value analysis of distance measurements to M87

Jiang Zhang,[1,2,3]★ Lingdou Li,[2] Han Su,[4] Yandong Chen[1]★ and Weibin Shi[5]★

[1]*School of Basic Sciences, Tianjin Agricultural University, Tianjin 300384, China*
[2]*Department of Mathematics and Physics, Hebei GEO University, Shijiazhuang 050016, China*
[3]*Hebei Key Laboratory of Optoelectronic Information and Geo-detection Technology, Hebei GEO University, Shijiazhuang 050016, China*
[4]*School of Statistics, Beijing Normal University, HaiDian District, Beijing 100875, China*
[5]*Shandong Provincial Key Laboratory of Optical Astronomy and Solar-Terrestrial Environment, School of Space Science and Physics, Shandong University at Weihai, Weihai 264209, China*

Accepted 2024 August 9. Received 2024 August 3; in original form 2024 April 9

ABSTRACT

We reanalyse the recent compilation of distance measurements to M87 by collecting the data from published literature. Different from the traditional statistical methods, based on the principle of minimum information loss, we use a robust most frequent value (MFV) procedure to estimate the distance to M87, irrespective of the Gaussian or non-Gaussian distributions. The MFV-based robust estimate for the M87 distance modulus is given by $31.09^{+0.04}_{-0.03}$ (statistical) $^{+0.05}_{-0.07}$ (systematic) mag corresponding to a 68.27 per cent confidence interval, whereas the result of combining the two uncertainties in quadrature is $31.09^{+0.06}_{-0.08}$ mag. We also construct the error distributions of M87 distance moduli values according to the weighted mean, median, and MFV, which is non-Gaussian. This demonstrates that the MFV method offers a more accurate and robust estimate of the distance to M87 compared to methods that depend on the unfulfilled assumption of Gaussianity.

Key words: methods: statistical – stars: distances – stars: statistics – cosmology: cosmological parameters.

1 INTRODUCTION

It is well known that the Virgo cluster, along with its giant elliptical galaxy M87, plays an important role in establishing the extragalactic distance ladder to more remote astronomical objects like the Fornax and Coma clusters. As an ideal candidate for the remote distance determination, M87 and its distance have been one of hot spots in a lot of research fields, from Hubble constant to black hole imaging (Event Horizon Telescope Collaboration 2019; Kim et al. 2020). Obviously, a more accurate value for the distance measurements to M87 will also improve our understanding of fundamental astrophysics and cosmology (de Grijs & Bono 2020; Mohan et al. 2024).

Because of the significant impact of the distance measurements to M87, there have been many distinct observational methods used to measure its value over the last several decades. After an extensive data mining effort, de Grijs and Bono (de Grijs & Bono 2020) (referred to as D20 hereafter) had compiled a data base of 211 distance measurements to M87/the Virgo cluster, whose result was $(m - M)_0 = 31.03 \pm 0.14$ mag corresponding to 16.07 ± 1.03 Mpc. In recent decades, there has been a notable increase in the accuracy of astronomical distance measurements, leading to a renewed focus on physical data research. None the less, the significant difference in distance measurements among the different methods remains a puzzling problem that has confounded researchers in the realms of physics and astrophysics. This has become a topic of much controversy (Ramakrishnan & Desai 2023).

The classical median method is widely used in statistical analysis to evaluate the characteristics of various observational quantities in a wide range of applications, as it is not influenced by outliers (Gott et al. 2001; Podariu et al. 2001; Chen & Ratra 2003; Chen, Gott & Ratra 2003; Chen & Ratra 2011; Crandall & Ratra 2014, 2015; Crandall, Houston & Ratra 2015; Bethapudi & Desai 2017; Camarillo et al. 2018a; Penton et al. 2018; Rajan & Desai 2018; Zhang 2018; Yu et al. 2020; Zhang et al. 2022; Ramakrishnan & Desai 2023; Rackers, Splawska & Ratra 2024). Several known examples of non-Gaussian error data have been used to apply median statistics concerning the Hubble constant (Chen et al. 2003; Chen & Ratra 2011), ^{7}Li abundance (Crandall et al. 2015; Zhang 2017), LMC and SMC distances (Crandall & Ratra 2015), deuterium abundance and spatial curvature constraints (Penton et al. 2018), the distance to the Galactic Centre (Camarillo et al. 2018a), galactic rotational velocity (Camarillo, Dredger & Ratra 2018b), and neutron lifetime (Rajan & Desai 2020). Likewise, another alternative approach is that of Bayesian statistics, as this is commonly utilized in astrophysics and particle physics (Von der Linden, Dose & Von Toussaint 2014; Sharma 2017; Rallapalli & Desai 2023; Rinaldi et al. 2023).

In particular, recently, the distance measurements to M87 have been thoroughly analysed using median statistics (Rackers et al. 2024). Besides, a similar meta-analysis has also been done (Ramakrishnan & Desai 2023). From the perspective of robust statistics, it is crucial to accurately estimate the distance to M87, taking into account the comprehensive nature of all observations. Even

★ E-mails: zhangphysics@126.com (JZ); 383876806@qq.com (YC); swb@sdu.edu.cn (WS)

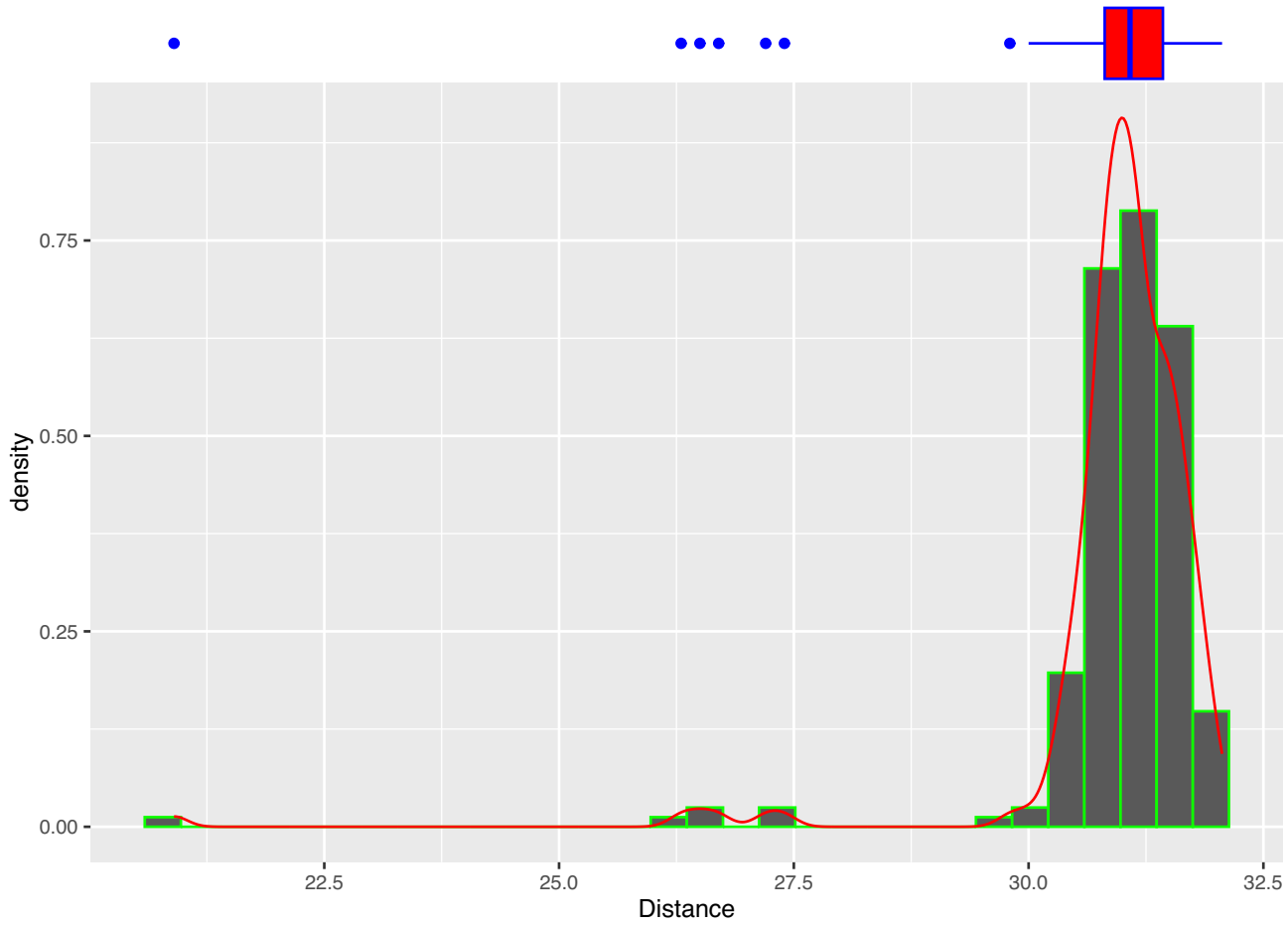

Figure 1. Histogram and probability density (red line) of the distance measurements to M87. [A colour version of this figure is available in the online version.]

though there has been extensive research on data analysis and uncertainty in physics and technology in recent decades, the existing discrepancies among different measurements still require new robust statistical methods to strengthen the robustness of the model. This has led us to utilize the MFV procedure to reanalyse this issue.

In this paper, we apply the MFV method (Steiner 1988, 1991, 1997; Steiner & Hajagos 2001; Kemp 2006; Szucs, Civan & Virag 2006; Szegedi 2013; Szegedi & Dobroka 2014; Szabó, Balogh & Stickel 2018; Zhang et al. 2022; Golovko 2023; Golovko, Kamaev & Sun 2023) to analyse the distance measurements to M87. The MFV method has been proposed to address the problems of lithium abundance, Hubble constant tension, and the neutron lifetime anomaly (Zhang 2017, 2018; Zhang et al. 2022). In particular, we aim to determine the robust best-fit estimate of distance to M87 given in D20. This work is organized as follows: In Section 2, we briefly summarize the data and descriptive statistics. Then, in Section 3, we analyse the methodology of MFV. Section 4 is dedicated to the description of the calculated results. By enhancing previous findings, we also computed the confidence intervals and demonstrated their superiority over traditional statistics using the most recent D20 compilation of the distance measurements to M87. Section 5 discusses the error distribution for distance measurements to M87. Furthermore, we show the comparison between theoretical MFV predictions and other statistical methods such as weighted mean and median. Eventually, our conclusions are given in Section 6.

2 DATA

Up to now, numerous observed values of the distance measurements to M87 using different techniques have been published. In our analysis, we use the D20 compilation including 15 tracers, such as Cepheids, planetary nebulae luminosity function (PNLF), surface brightness fluctuations (SBF), tip of the red giant branch (TRGB) magnitude, and novae (de Grijs & Bono 2020) (The original measurements data set sorted by tracer type can be seen at http://astro-expat.info/Data/pubbias.html). Further details of D20 data set had been discussed in the recent literature, e.g. Refs. (Ramakrishnan & Desai 2023; Rackers et al. 2024). Ultimately, in this paper, we use 211 independent measurements of the distance to M87 to analyse following Rackers et al. (2024).

We adopt descriptive statistics methods to analyse the data of the distance measurements to M87 and plot histograms of the number of data values, as shown in Fig. 1. Using ggplot2, 30 bins were chosen. Based on the grammar of graphics elucidating the essential elements that form the basis of all statistical graphics, the histogram figure describes a mapping from the data to the aesthetic feature of geometric objects (Wilkinson 2005; Wickham 2010). When the number of bins is different, the bars will start from a bin with the specified bin width. Despite the changes in the numerical values of the histogram bins, the holistic trend of the graph remains unchanged (Podariu et al. 2001; Wickham 2016). Also, the measurements are illustrated in a boxplot in the upper row, and the median is represented by the line in the middle of the boxplot. Extending from the edges

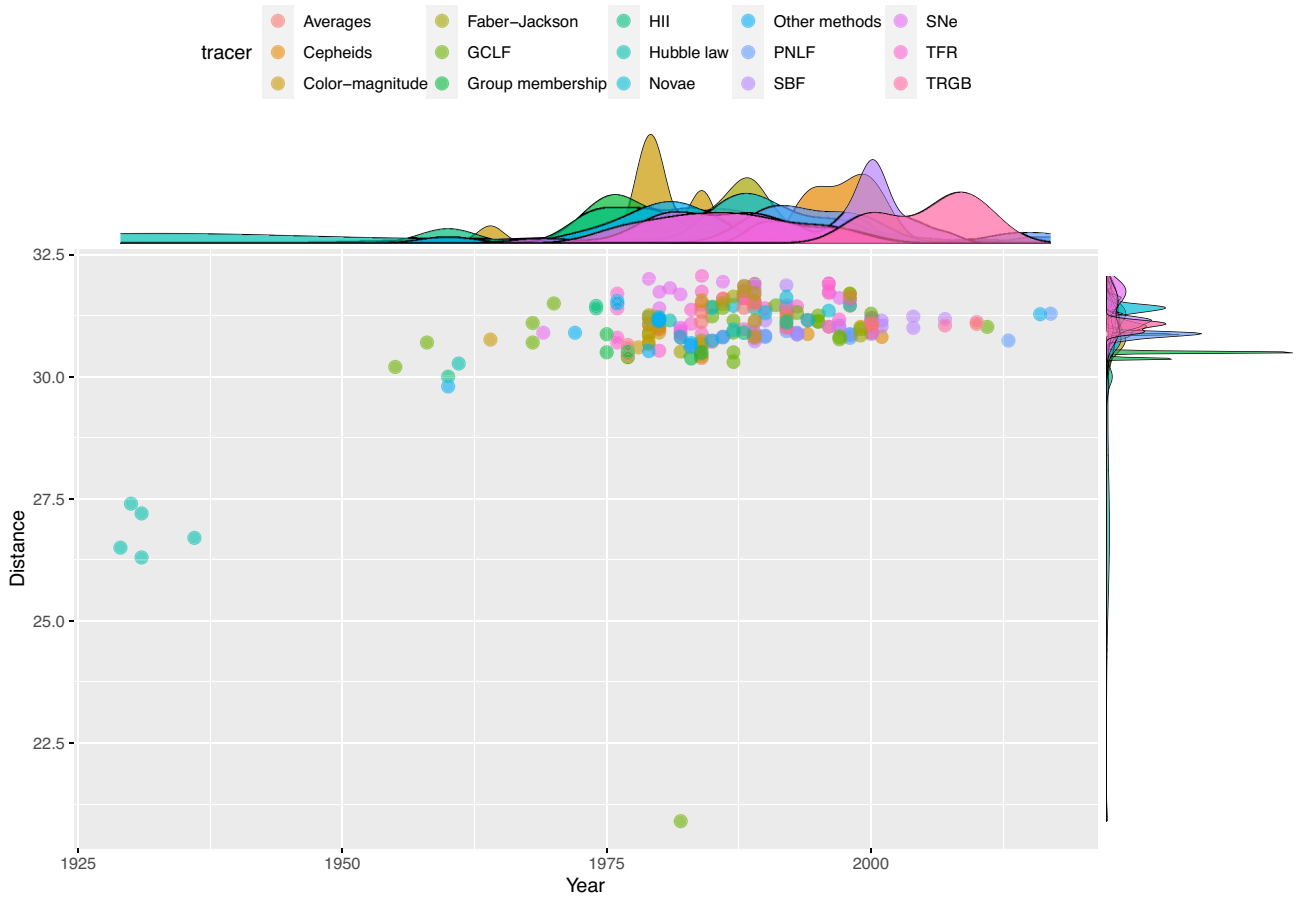

Figure 2. Published distance measurements to M87 as a function of publication date. The taxonomic approach of the distance measurements to M87 for analysis is similar to that of D20. [A colour version of this figure is available in the online version.]

of the boxplot are the whiskers corresponding to the 25 and 75 per cent quantiles of the distribution. Apart from the whiskers, there are individual outliers present, which are points that are deemed to be significantly distinct from the rest of the sample.

Fig. 2 illustrates publication years with the distance measurements to M87 used for analysis since 1929, including tracers listed in D20 following the taxonomic approach of D20 (de Grijs & Bono 2020). Moreover, the marginal panels associated with the main panel show the marginal distribution of the distance measurements to M87 as the function of the distance or publication data. The points represent the overall data set in different colours corresponding to different individual tracers. With the view of vertical comparison, Fig. 3 shows a ridge graphical representation of the distance measurements to M87 based on different methods from different tracers. As depicted in the plots above, we can see some apparent relationships between our quantitative variables. In short, for the purpose of a holistic comparison from multiple perspectives, these figures display the comprehensive graphical representation of the distance measurements to M87 based on different methods from various individual tracers.

It is worthwhile to investigate the different deviations of the distance measurements to M87 mentioned in D20 from the heteroscedasticity. When dealing with all of the collected data, it is essential to address zero error and asymmetric systematic uncertainties in a clear and consistent manner. However, accurately evaluating the impact of zero error and asymmetric uncertainties remains a challenging task (Barlow 2003; Audi et al. 2017; Barlow 2021). The main reason is that the anomalous deviation among different measurement methods of M87 may be attributed to unidentified systematic effects and uncertainties, potentially indicating the necessity of robust MFV statistics. On the other side, the physical measurement is approximation for true value and cannot be with zero error. Analogous statistical procedures have been discussed using the more general Bayesian/frequentist framework to deal with possible unknown systematic effects (Cowan 2019; Erler & Ferro-Hernández 2020). Therefore, in order to reduce the sensitivity to outliers, we use the average value of the uncertainties to calculate the error distribution for the weighted mean in the case of zero error (Rackers et al. 2024).

3 ANALYSIS OF METHODOLOGY

From a distance ladder perspective, the estimation of the distance measurements to M87 is one of the vital problems (de Grijs & Bono 2020). In order to obtain a more accurate estimate of measurements, there has been a substantial application of statistical methods, including median statistics, maximum likelihood estimation, and Bayesian statistics (Feigelson & Babu 2012). Understandably, there is no justification for researchers to perpetually suppose that the prior distribution of a physical quantity is normal. Although Gaussian distribution is commonly used based on the central limit theorem, it is not always the most suitable choice, particularly when dealing with special samples. For example, there are exceptions to the central limit

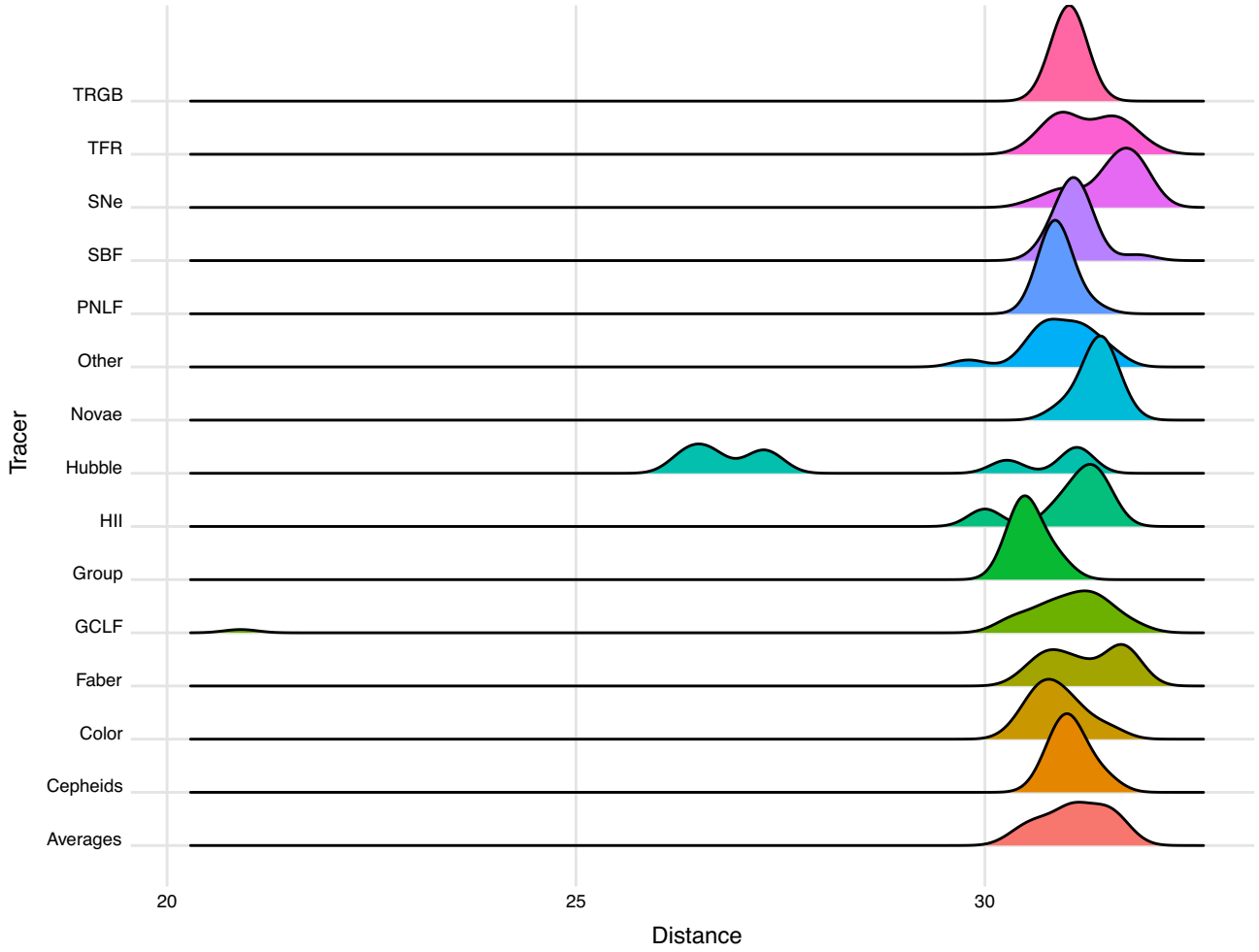

Figure 3. The ridge plot of the observed results used for the analysis from different tracers. [A colour version of this figure is available in the online version.]

theorem in the case of a random variable following a Cauchy distribution. Another significant issue is the heavy-tailed problem shown in the observed distributions. To be honest, it is extremely difficult for anyone to accurately determine if the normality characteristic is intrinsic to the measurement data (Chen et al. 2003; Crandall et al. 2015; Singh et al. 2016; Bailey 2017; Zhang 2017).

When analysing measurement data, χ^2 analyses, the least squares method (LSM; Kelly 2007; Zhang et al. 2012), and median statistics are commonly given priority consideration to extract important information (Gott et al. 2001). However, when the prior distributions are non-Gaussian, it is necessary to consider more specific details of the prior distributions in order to achieve more precise and robust outcomes. On the other hand, as is known to all that every computational statistical model contains inevitable underlying assumptions. Clearly, before performing any statistical computation, it is essential to consider the normality of the distribution, which encompasses the error distribution and the prior distribution (Zhang 2017; Zhang et al. 2022). Moreover, dealing with heteroscedasticity is consistently a major challenge for traditional methods. Therefore, it is important to use a violin plot to reveal the significant details regarding the distributions of the distance measurements to M87, as shown in Fig. 4. The violin and kernel density plots for different methods are shown in these subgraphs, which are particularly useful for evaluating summary and descriptive statistics. Additionally, we can make a direct comparison between the median and average values, allowing us to intuitively observe the distributions of various subgroups and the potential non-Gaussian errors in the distance measurements to M87 from different approaches. In brief, these obstacles also inspire us to utilize the novel MFV method for determining the distance to M87.

On the basis of the central limit theorem, the distribution of measurement data should be normal in most cases. Even so, the error distributions of measurement data are still probably non-Gaussian. For instance, it is possible that the measurement data might not originate from a random sample of independent, identically distributed random variables, which should be proven. Due to the ideal conditions of pure mathematics, it is necessary to temporarily accept some plausible hypotheses based on expediency. According to the data of distance measurements to M87, physicists expect to accurately estimate the real value from different prior distributions. For the sake of a better implementation of this purpose, Steiner (Steiner 1991, 1997) proposed a more robust statistical algorithm–MFV method, based on the principle of minimizing information loss. Regardless of whether the prior distribution is considered to be Gaussian or not, the robust MFV procedure is not only highly efficient but also eliminates shortcomings such as high sensitivity to outliers in the data set for measurements (Zhang 2017, 2018).

In order to elucidate the effect of prior distribution and error distributions, we utilize the MFV procedure to assess the characteristics of the data set of distance measurements to M87. Unlike traditional

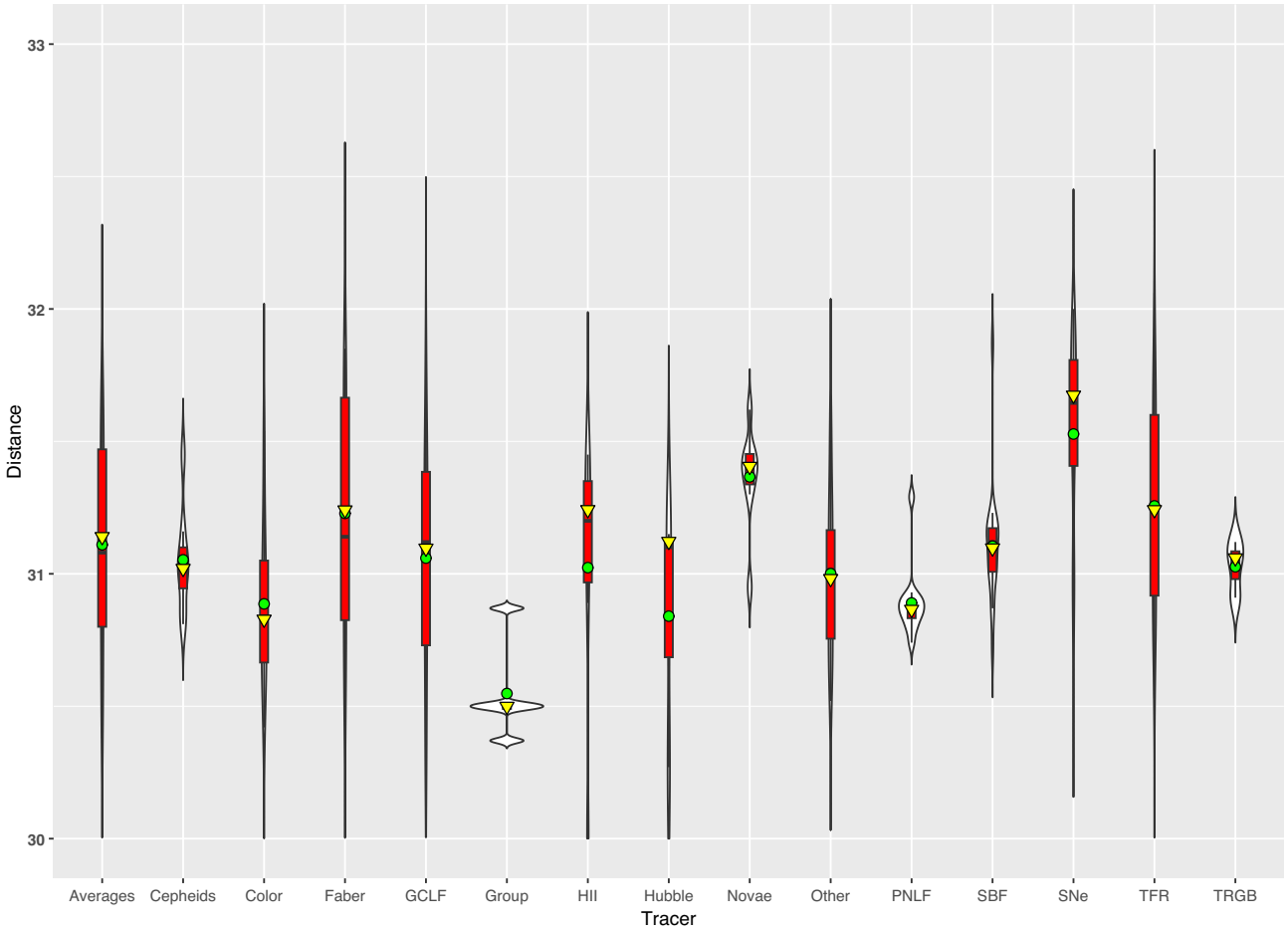

Figure 4. Violin plots and nested box diagrams of distance measurements to M87. The MFV and average values from different methods are indicated by the inverted triangle and circle, respectively, while the solid horizontal line in the box illustrates the median. [A colour version of this figure is available in the online version.]

methods such as maximum likelihood estimation or LSM, Steiner put forward the maximum reciprocals principle,

$$\sum_i \frac{1}{X_i^2 + S^2} = \max, \tag{1}$$

where X_i is the residuals and deviations, and S denotes the measurement error. According to the minimization of the information divergence (relative entropy) demonstrating the measure of information loss (Huber 1981; Steiner 1991, 1997), Steiner suggested the MFV method and the scaling factor ε, i.e. dihesion, for the sake of evaluating the parameter of scale to some extent to reduce the information loss. Furthermore, we can calculate the MFV and the dihesion via iterations. After the $(j + 1)$-th step of the MFV procedure, the relative equation of iterations for the most frequent value M is as follows:

$$M_{j+1} = \frac{\sum_{i=1}^{n} \frac{\varepsilon_j^2 x_i}{\varepsilon_j^2 + (x_i - M_j)^2}}{\sum_{i=1}^{n} \frac{\varepsilon_j^2}{\varepsilon_j^2 + (x_i - M_j)^2}}, \tag{2}$$

where x_i is a series of the measurements and the dihesion ε_j can be calculated by

$$\varepsilon_{k+1}^2 = \frac{3\sum_{i=1}^{n} \frac{\varepsilon_k^4 (x_i - M_j)^2}{\left[\varepsilon_k^2 + (x_i - M_j)^2\right]^2}}{\sum_{i=1}^{n} \frac{\varepsilon_k^4}{\left[\varepsilon_k^2 + (x_i - M_j)^2\right]^2}}. \tag{3}$$

Where the iterative initial value M_0 is chosen as the average value of the measurements, and the initial value of ε is obtained as

$$\varepsilon_0 = \frac{\sqrt{3}}{2}(x_{\max} - x_{\min}). \tag{4}$$

Additionally, we utilize the fixed threshold criterion to control precision during iterations. After a number of iterations, the most frequent value M and dihesion ε can be determined when the parameter uncertainty is below a certain threshold (e.g. 10^{-5}). Evidently, the robust dihesion ε does not behave like the sensitive standard deviation in LSM, which is easily affected by outliers (Steiner 1991, 1997).

4 RESULTS

The outcome of these calculations is MFV = 31.09 mag, which is in agreement with the recently published results (31.08 mag) (Ramakrishnan & Desai 2023; Rackers et al. 2024). Because observational data reflect the essence of physical quantities, it is possible to use robust statistics and data science, such as the MFV method, to characterize the data. For estimating the uncertainty of physical

Table 1. MFV and medians of distance measurements to M87 by tracer.

tracers	Number	MFV	$\text{shift}_{\text{mfv}}$	95 per cent c.l.	range	Median	$\text{shift}_{\text{med}}$	95 per cent c.l.	range
All data	211	31.09	0	31.02–31.17	0.15	31.08	0	31.02–31.15	0.13
Averages	21	31.14	0.05	30.92–31.38	0.46	31.08	0	30.98–31.40	0.42
Cepheids	7	31.02	−0.07	30.86–31.20	0.34	31.02	−0.06	30.87–31.16	0.29
Colour-magnitude	11	30.83	−0.26	30.64–31.06	0.42	30.84	−0.24	30.66–31.06	0.4
Faber–Jackson	11	31.24	0.15	30.8–31.70	0.9	31.14	0.06	30.81–31.69	0.88
GCLF	32	31.09	0.00	30.88–31.29	0.41	31.11	0.03	30.83–31.27	0.44
Group membership	5	30.50	−0.59	30.37–30.87	0.5	30.5	−0.58	30.37–30.87	0.5
H II	6	31.24	0.15	30.54–31.45	0.91	31.2	0.12	30.45–31.43	0.98
Hubble law	8	26.96	−4.13	26.38–31.12	4.74	27.3	−3.78	26.5–31.10	4.6
Novae	8	31.41	0.32	31.3–31.47	0.17	31.4	0.32	31.3–31.46	0.16
Other methods	15	30.96	−0.13	30.71–31.18	0.47	30.9	−0.18	30.69–31.15	0.46
PNLF	12	30.87	−0.22	30.82–30.90	0.08	30.865	−0.215	30.83–30.9	0.07
SBF	18	31.10	0.01	31.01–31.18	0.17	31.12	0.04	31.02–31.17	0.15
SNe	18	31.67	0.58	31.4–31.82	0.42	31.645	0.565	31.43–31.80	0.37
TFR	36	31.24	0.15	30.97–31.47	0.5	31.235	0.155	30.98–31.49	0.51
TRGB	3	31.06	−0.03	30.91–31.12	0.21	31.05	−0.03	30.91–31.12	0.21

quantities, the bootstrap method is one of the most effective methods and is essential for evaluating the rationality of the calculated results (Efron & Tibshirani 1994; Davison & Hinkley 1997). In order to calculate the confidence interval, the bootstrap method follows a fundamental process. Assuming that the observed data set of distance measurements to M87 is $(d_1, \ldots, d_i)$ chosen from an independent and identical distribution of true values of distance measurements with the corresponding statistic $\theta(d_1, \ldots, d_i)$, i.e. the MFV. Once a bootstrap sample $(d_1^*, \ldots, d_i^*)$ has been generated from the initial observed data with replacement, the next step is to calculate the important statistic, MFV, for the bootstrap sample. By repeating this process B times (usually 1000–3000 times), the distribution of the MFV is generated. As a result, these distributions can be employed to assess confidence intervals (typically 68.27 or 95.45 per cent) of the MFV for different distance measurement techniques. Finally, the calculated 68.27 per cent confidence interval for all measurements is [31.06, 31.13] mag, taking into account statistical bootstrap errors, while the calculated 95.45 per cent confidence interval for all data is [31.02, 31.17] mag.

Generally, there are three statistical central estimates: median, weighted mean (Podariu et al. 2001), and MFV. As a comparison, using median statistics is another way to estimate confidence intervals for the distance measurements to M87 (Gott et al. 2001; Camarillo et al. 2018a). From the order statistic perspective, according to the binomial test and estimation in non-parametric statistics (Conover 1999), the probability of the median between values $x^{(r)}$ and $x^{(s)}$ is

$$p(x^{(r)} \leqslant \text{median} \leqslant x^{(s)}) = p(\text{median} \leqslant x^{(s)}) - p(\text{median} < x^{(r)}),$$

$$= \sum_{i=r}^{s} \binom{n}{i} / 2^n, \tag{5}$$

where $x^{(i)}$ is the order statistic. By application of this formula, the median for all measurements is 31.08 and the calculated 68.27 per cent confidence interval is [31.03, 31.12] mag, while the 95.45 per cent confidence interval for all data is [31.02, 31.15] mag.

The calculated results and D20 data for the distance measurements to M87 are listed in Table 1, which are used in our analysis. We group the 211 measurements into 15 subgroups based on the tracer type in the final D20 compilation. The number of each subgroup and the corresponding MFV and median statistics results are shown in Table 1. The shifts in the 4th and 8th columns of the table list the systematic displacement of MFV and median between the total data set and subsets. The ranges in the 6th and 10th columns are calculated by finding the distance between the upper and lower limits. From a theoretical perspective, the definition of this range varies depending on the type of fundamental uncertainty. In the case of measured or binned scales, the measurement space can be described as the relative standing of the observed data sets, allowing for the definition of limits through two specified percentile endpoints or z-scores (Chakraborti & Li 2007; Mendenhall & Sincich 2016). Thus, both the upper and lower limits correspond to the dispersion of the data, which are determined as the difference between the higher and lower percentiles of the 95 per cent confidence level (C.L.) under typical conditions (Chen & Ratra 2011; Ialongo 2019; Zahedy et al. 2021). Furthermore, Fig. 5 shows histograms for all tracer subgroups, demonstrating multiple panel plots in terms of the individual tracer facets. The main goal is to explore the statistical frequent characteristic as a function of subgroups.

There exist two primary categories of experimental errors: systematic and statistical. In fact, it is very difficult to reveal the presence of systematic errors through the variability in measurements. No theory or model exists that adequately handles uncertainties caused by systematic errors in a consistent manner (D'agostini 2003; Barlow 2021). The only established principle regarding systematic errors is that they must be recognized and mitigated to a degree well below the required precision (Audi et al. 2012; Taylor 2022). Due to the complexity involved in offering a rigorous proof, we estimate systematic errors following Chen & Ratra (2011) and Rackers et al. (2024). Inspired by the classic idea of generalization in statistical learning (Hastie et al. 2009; James et al. 2023), our goal is to strike a good balance between statistical methods and practical measurement experience according to the principle of Occam's razor. Following Chen & Ratra (2011), with the ongoing debates surrounding systematic errors in the error analysis field, we can consider subgroup systematic uncertainties as pseudorandom errors at the level of the entire list (Gott et al. 2001).

Statistical uncertainty exists within each tracer subgroup, leading to measurement variability, while systematic errors may arise among tracers due to variations in techniques and calibrations. We have compiled a novel data set comprising the MFV values of individual tracer subgroups. Similar to Chen & Ratra (2011) and Rackers et al. (2024), a median statistical analysis is carried out on this new data set to determine the median of MFVs and quantify its associated uncertainty. In the scenario where we consider these medians to differ

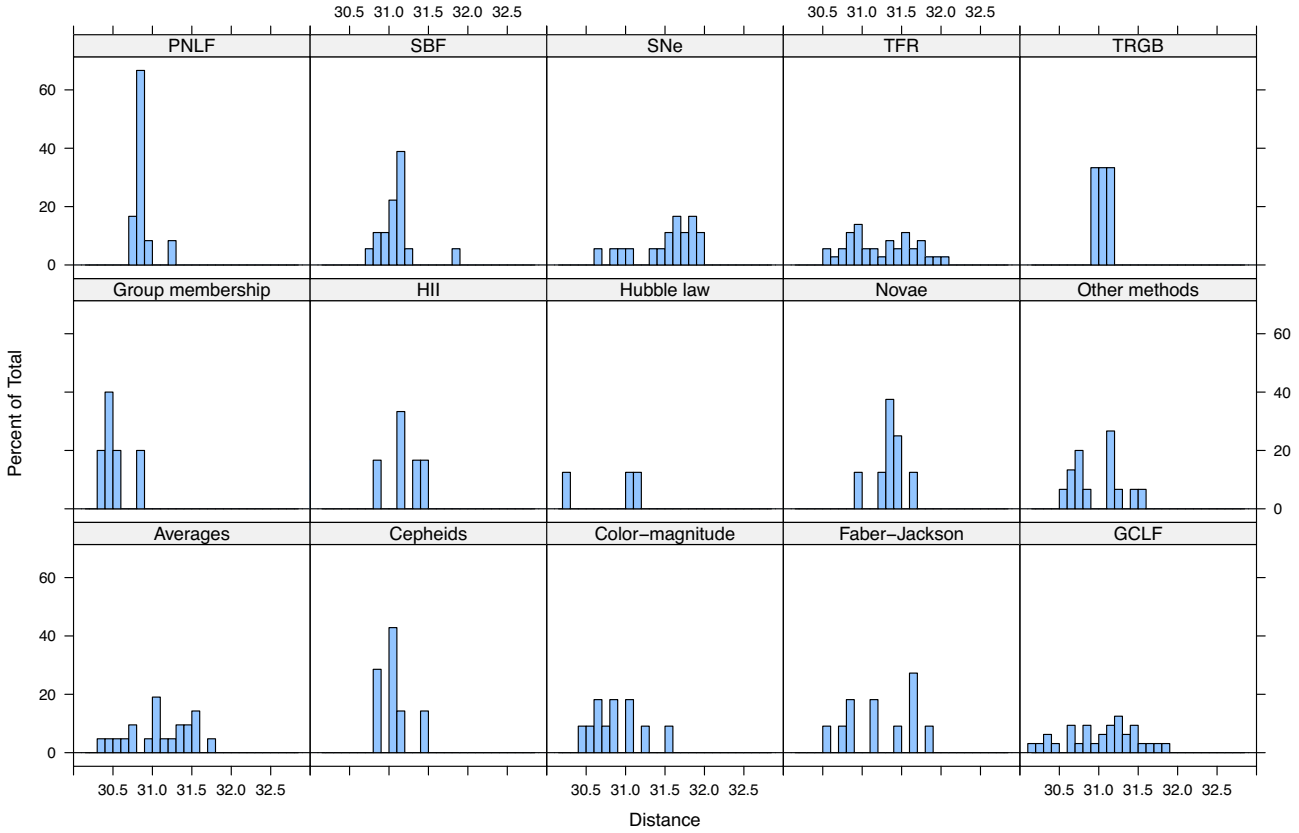

Figure 5. Distributions of the distance measurements to M87 from different subgroups. Each heading lists the tracer type. Only measurements in the (horizontal axes) range of 30–33 mag are displayed, but this limitation does not affect the holistic impression about the distribution of different individual tracers. [A colour version of this figure is available in the online version.]

solely in a systematic manner, the resulting uncertainty corresponds to the systematic uncertainty present in the entirety of the tracers (Gott et al. 2001; Chen & Ratra 2011).

Therefore, we can apply these 15 subgroup MFVs in Table 1 as a new data set to estimate the systematic uncertainty of whole group of tracers. For the sake of simplicity, we use median statistics to obtain the median of these subgroup MFVs and its relevant uncertainty. The result is $31.09^{+0.05}_{-0.07}$ (systematic) mag at 68.27 per cent significance. We also combine the statistical and systematic errors in quadrature to get $31.09^{+0.06}_{-0.08}$, which is consistent with the results of recent references (Ramakrishnan & Desai 2023; Rackers et al. 2024). Besides, based on binomial distribution, we used median statistics to analyse subgroup medians and our results are consistent with those in recent references (Ramakrishnan & Desai 2023; Rackers et al. 2024)

5 DISCUSSION

It holds meaning to explore the distributions of deviations of the distance measurements to M87 mentioned in D20 from the central estimate. The present work outlines three strategies for statistical central estimation: weighted mean (Podariu et al. 2001), median, and MFV. The weighted mean is defined as

$$D_{\rm wm} = \frac{\sum_{i=1}^{N} D_i/\sigma_i^2}{\sum_{i=1}^{N} 1/\sigma_i^2}, \tag{6}$$

where D_i denotes the measurement of distance and σ_i is the one standard deviation error, i.e. the quadrature sum of the statistical and systematic uncertainties. The weighted mean standard deviation is

$$\sigma_{\rm wm} = \frac{1}{\sqrt{\sum_{i=1}^{N} 1/\sigma_i^2}}. \tag{7}$$

The goodness of fit χ^2 is

$$\chi^2 = \frac{1}{N-1}\sum_{i=1}^{N}(D_i - D_{\rm wm})^2/\sigma_i^2. \tag{8}$$

The number of standard deviations that χ deviates from unity (Farooq, Crandall & Ratra 2013; Crandall & Ratra 2014, 2015) is described by

$$N_\sigma = |\chi - 1|\sqrt{2(N-1)}. \tag{9}$$

By utilizing the median as well as MFV statistics approaches, we can construct the error distributions. Just like how median statistics assume statistical independence of all measurements, the MFV statistics also do not take into account individual measurement uncertainties. This results in a broader range of errors on the central value compared to the weighted mean technique. In accordance with the specified central estimate of all measurements, the error distribution linked to standard deviations (Crandall & Ratra 2015; Penton et al. 2018; Camarillo et al. 2018a) is described by

$$N_{\sigma_i} = \frac{D_i - D_{\rm CE}}{\sqrt{\sigma_i^2 + \sigma_{\rm CE}^2}}, \tag{10}$$

where $D_{\rm CE}$ is the central estimate of distance measurements, either the median $D_{\rm med}$ or MFV $D_{\rm MFV}$, and $\sigma_{\rm CE}$ is the uncertainty of $D_{\rm CE}$,

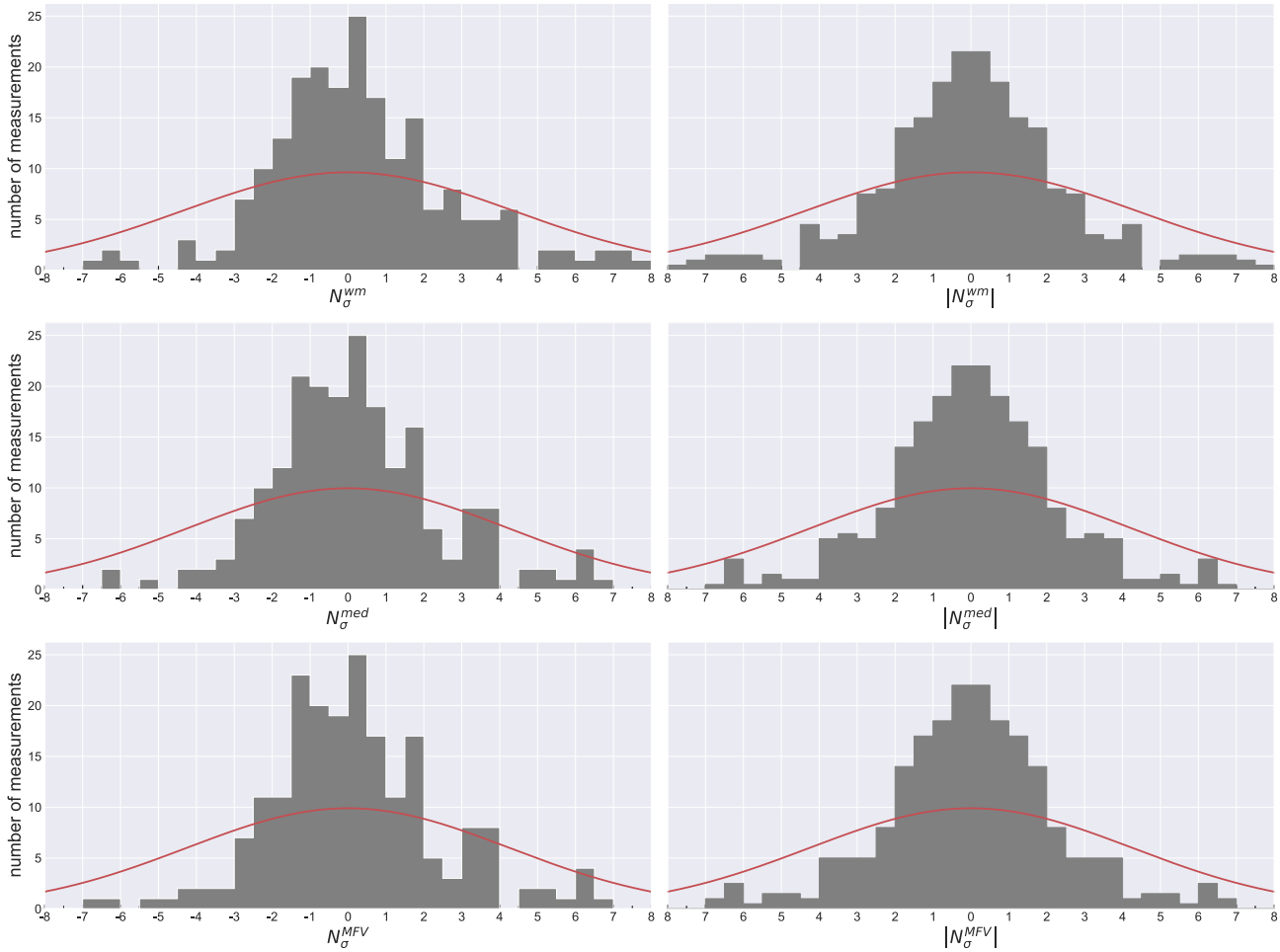

Figure 6. Histograms of the number of standard deviations in half bins away from the weighted mean, median, and MFV listed in the top, middle, and bottom rows. The left (right) column illustrates the signed (absolute) deviation, where the smooth curves in panels represent the best-fit Gaussian. The N_σ of positive and negative cases indicate greater and less than the weighted mean, median, and MFV. [A colour version of this figure is available in the online version.]

either $\sigma_{\rm med}$ or $\sigma_{\rm MFV}$. Noteworthy, this formula presupposes that the central estimate is uncorrelated with the data set, which is not fulfilled in this scenario. Although there is an expression for Gaussianly distributed data and for a weighted-mean central estimate (See the Appendix of Camarillo et al. 2018a), the accurate expressions in the case of non-Gaussian distributions still remain unresolved for the important statistics such as median and MFV. When the central estimate $D_{\rm CE}$ is the true value, this formula is always correct in a frequentist framework. Taking into account, the statistic as an approximation to the true value, from the consistency of comparison, we use the derived equations to simplify the analysis, which provides valuable holistic inferences. These various combinations of central estimates and uncertainties are given by

$$N_{\sigma_i}^{\rm wm} = \frac{D_i - D_{\rm wm}}{\sqrt{\sigma_i^2 + \sigma_{\rm wm}^2}}, \tag{11}$$

$$N_{\sigma_i}^{\rm med} = \frac{D_i - D_{\rm med}}{\sqrt{\sigma_i^2 + \sigma_{\rm med}^2}}, \tag{12}$$

$$N_{\sigma_i}^{\rm MFV} = \frac{D_i - D_{\rm MFV}}{\sqrt{\sigma_i^2 + \sigma_{\rm MFV}^2}}. \tag{13}$$

de Grijs & Bono (2020) reported a distance modulus of $(m - M)_0^{M87} = 31.03 \pm 0.14$ mag. They only chosed a well-calibrated and independently determined subset from the Cepheids, TRGB, and SBF measurements. Similar to previous work in Ramakrishnan & Desai (2023), for the weighted mean we used the measurements with error bars and obtained $(m - M)_{\rm wm} = 31.109 \pm 0.008$ mag. Also, we find $\chi^2 = 6.57$ and the number of standard deviations that χ deviates from unity is 28.83. Moreover, based on the procedure outlined in Rackers et al. (2024), we use the full data set for calculations by setting the measurements without errors to the average value of the uncertainties for that tracer. The weighted mean of all 15 tracers is $(m - M)_{\rm wm} = 31.068 \pm 0.008$ mag. These results are in good accord with previous work (Ramakrishnan & Desai 2023; Rackers et al. 2024)

The MFV and median statistics procedures are advantageous because they do not rely on the individual measurement errors. As a result, a greater uncertainty will be observed in the central estimate compared to the weighted mean scenario. When applying median and MFV statistics to construct the confidence interval via the above equations, the central estimate for $D_{\rm med}$ is $31.08^{+0.04}_{-0.05}$ mag, with a 1σ range of [31.03, 31.12]. The MFV estimate is given by $D_{\rm MFV} = 31.09^{+0.04}_{-0.03}$ mag with uncertainty corresponding to 68.27 per cent confidence intervals.

By employing these statistical methods, we are able to visualize the error distributions of distance measurements with respect to N_σ (Crandall & Ratra 2015), equations (10)–(13), in Fig. 6, which indicates the N_σ and symmetrical $|N_\sigma|$ histograms using the weighted

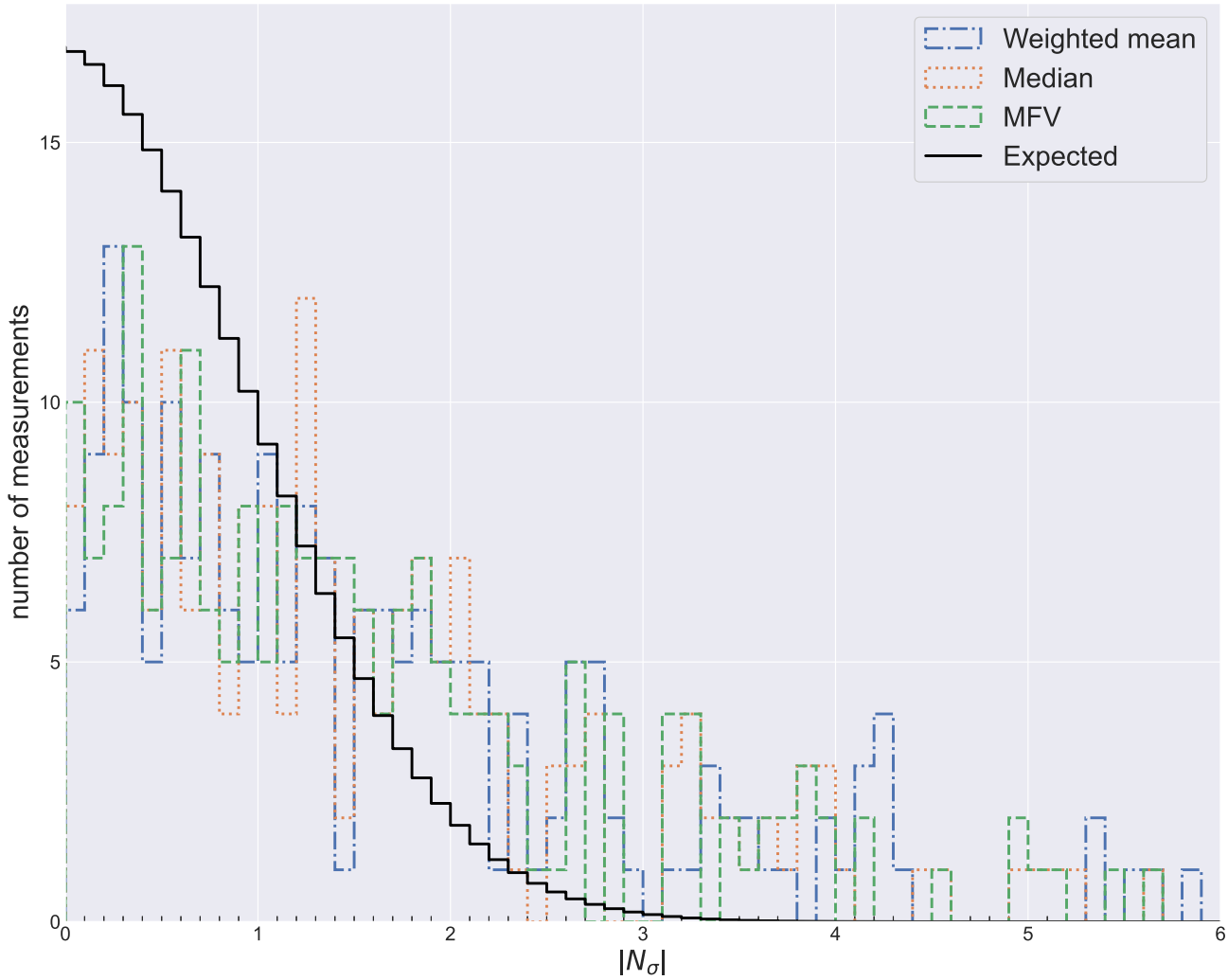

Figure 7. Histogram of the error distribution in $|N_\sigma| = 0.1$. The solid black line indicates the expected Gaussian probabilities for all data and the dash–dotted, dash, and dot lines denote the numbers of $|N_\sigma|$ values for the weighted mean, MFV, and median, respectively. [A colour version of this figure is available in the online version.]

mean, median, and MFV. The histogram of error distributions of the measurements is displayed in Fig. 7 with $|N_\sigma| = 0.1$ bin size for a more specific viewpoint. Clearly, these figures show that the weighted mean case has a broader range than the expected Gaussian distribution.

From these graphs, we can observe numerous statistical characteristics. The expected Gaussian distribution is expected to yield 10 values with $|N_\sigma| \geq 2$ and a single value with $|N_\sigma| \geq 3$. But for the weighted mean case, there are 73 values with $|N_\sigma| \geq 2$, 42 with $|N_\sigma| \geq 3$, and 29 with $|N_\sigma| \geq 4$. Remarkably, 68.3 per cent of the $N_{\sigma_{\rm wm}}$ error distribution lies within $-2.06 \leq N_\sigma \leq 2.14$ while 95.4 per cent falls within $-19.85 \leq N_\sigma \leq 5.51$. The observed $N_{\sigma_{\rm wm}}$ error distribution has constraints of $|N_\sigma| \leq 2.13$ and $|N_\sigma| \leq 6.86$, respectively, and 37.9 and 65.4 per cent of the values lie within $|N_\sigma| \leq 1$ and 2, respectively.

For the median case, the distribution has a narrower tail than the expected Gaussian distribution, with 68 values of $|N_\sigma| \geq 2$, 42 with $|N_\sigma| \geq 3$ and 21 with $|N_\sigma| \geq 4$. For signed N_σ, 68.3 per cent of the data lie within $-1.93 \leq N_\sigma \leq 2.04$, while 95.4 per cent fall within $-15.70 \leq N_\sigma \leq 6.16$. The absolute $|N_\sigma|$ error distribution has constraints of $|N_\sigma| \leq 2.03$ and $|N_\sigma| \leq 6.38$, respectively. Moreover, 38.9 and 67.8 per cent of the values lie within $|N_\sigma| \leq 1$ and 2, respectively.

On the other hand, for the MFV case, we gain a central estimate of $(m - M)_{\rm MFV} = 31.09$ mag, see Figs 6– 7, and also find a non-Gaussian error distribution with 68 values of $|N_\sigma| \geq 2$, 42 with $|N_\sigma| \geq 3$ and 22 with $|N_\sigma| \geq 4$. 68.3 per cent of the data falls within $-1.96 \leq N_\sigma \leq 2.05$, while 95.4 per cent lie within $-6.59 \leq N_\sigma \leq 6.32$. The $|N_\sigma|$ error distribution has constraints of $|N_\sigma| \leq 2.02$ and 6.48, respectively, and 38.4 and 67.8 per cent of the values fall within $|N_\sigma| \leq 1$ and 2, respectively.

It is evident from these data analysis that the error distribution for the MFV case is similar to that of the median case, while being narrower than that of the weighted mean case. The progressively tightening distributions of the weighted mean, median, and MFV could potentially be associated with unaccounted-for systematic uncertainties or correlations among distance measurements to M87, which have not been taken into consideration (de Grijs, Wicker & Bono 2014; Crandall & Ratra 2015; de Grijs & Bono 2020). Evidently, these in-depth statistical descriptions show that the error distributions of the weighted mean, median, and MFV are non-Gaussian, underscoring the effectiveness of the MFV technique

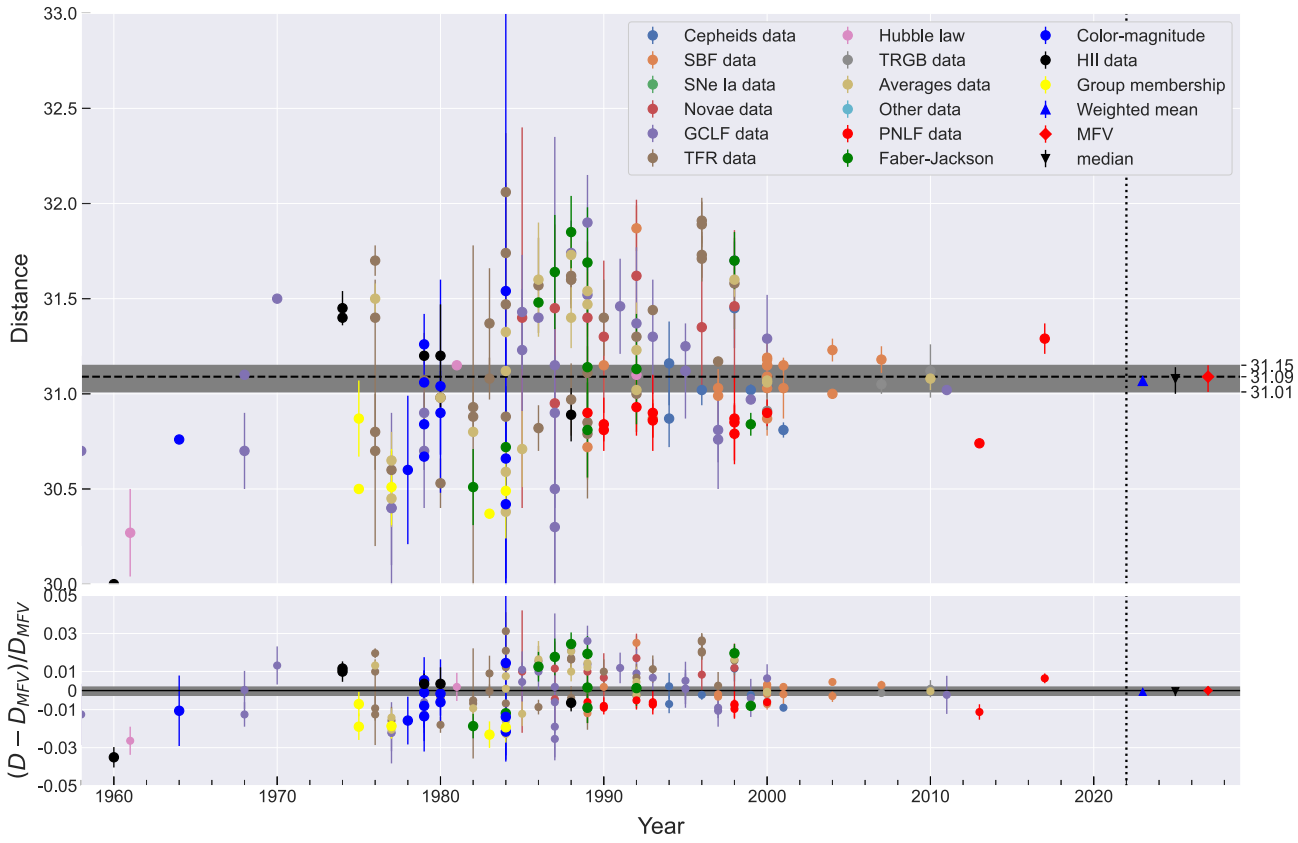

Figure 8. (Top) The distance measurements to M87 as a function of the publication year. The points represent the measured data using different methods, while the triangle, diamond, and inverted triangle depict the weighted mean, MFV, and median, respectively. Dark grey shadings indicate the MFV uncertainties are at 1σ confidence level. (Bottom) We show the residuals of the fit or data with respect to the MFV as a function of the publication date. [A colour version of this figure is available in the online version.]

for a robust analysis of distance measurements to M87. In Fig. 8, we apply equations of three statistical methods to plot the distributions of measurements illustrated as a function of years, which demonstrates the calculated results using the weighted mean, median, and MFV represented by different symbols. The bottom panel displays the calculated residuals $\triangle D/D_{\rm MFV}$ from the MFV. As mentioned previously, similar results were obtained in the references (Ramakrishnan & Desai 2023; Rackers et al. 2024). This strongly indicates that error distributions are not Gaussian, which in turn supports the reliability and reasonableness of MFV estimate.

6 CONCLUSION

In brief, the problem of the long-standing discrepancy in the distance measurements to M87 remains a crucial challenge in the study of astrophysics and cosmology. Despite the non-Gaussian nature of the measurement compilation, we utilized the MFV statistics technique to reconstruct a comprehensive statistical analysis of the data set for the distance measurements to M87, which contain different tracer types. In terms of robustness to the observed data, the MFV estimate is given by $31.09^{+0.04}_{-0.03}$(statistical)$^{+0.05}_{-0.07}$ (systematic) mag corresponding to a 68.27 per cent confidence interval, whereas the result of combining the two uncertainties in quadrature is $31.09^{+0.06}_{-0.08}$ mag. According to the binomial distribution, the median statistical analysis yields $31.08^{+0.04}_{-0.05}$(statistical) $^{+0.04}_{-0.06}$(systematic) mag at 68.27 per cent significance. Moreover, based on the weighted mean, median and MFV, we construct the error distributions of distance measurements to M87 and find the characteristic of the non-Gaussianity. The consistent results have shown the effectiveness and robustness of MFV statistics, which will encourage more exploration into the use of the MFV method in analogous scenarios.

ACKNOWLEDGEMENTS

We greatly appreciate the anonymous referee for their careful reading and valuable comments. We thank Z.-W Han, B. Zhang, E. Feigelson, and G.-R Li for valuable discussions. This work was supported by the National Natural Science Foundation of China (Grant No. 11547041, 11403007, 11701135, 11673007), the Natural Science Foundation of Hebei Province (A2017403025, A2021403002).

DATA AVAILABILITY

The data underlying this article are available in the article and the cite references.

REFERENCES

Audi G., Wang M., Wapstra A. H., Kondev F. G., MacCormick M., Xu X., Pfeiffer B., 2012, Chin. Phys. C, 36, 1287
Audi G., Kondev F. G., Wang M., Huang W. J., Naimi S., 2017, Chin. Phys. C, 41, 030001
Bailey D. C., 2017, R. Soc. Open Sci., 4, 160600
Barlow R., 2003, preprint(arXiv:physics/0306138)
Barlow R. J., 2021, CERN Yellow Rep. School Proc., 5, 197

Bethapudi S., Desai S., 2017, Eur. Phys. J. Plus, 132, 78
Camarillo T., Mathur V., Mitchell T., Ratra B., 2018a, PASP, 130, 024101
Camarillo T., Dredger P., Ratra B., 2018b, Ap&SS, 363, 268
Chakraborti S., Li J., 2007, Am. Stat., 61, 331
Chen G., Ratra B., 2003, PASP, 115, 1143
Chen G., Ratra B., 2011, PASP, 123, 1127
Chen G., Gott J. R., Ratra B., 2003, PASP, 115, 1269
Conover W. J., 1999, Practical Nonparametric Statistics. John Wiley and Sons, New York, NY, USA
Cowan G., 2019, Eur. Phys. J. C, 79, 133
Crandall S., Ratra B., 2014, Phys. Lett. B, 732, 330
Crandall S., Ratra B., 2015, ApJ, 815, 87
Crandall S., Houston S., Ratra B., 2015, Mod. Phys. Lett. A, 30, 1550123
D'agostini G., 2003, Bayesian reasoning in data analysis: A critical introduction. World Scientific, London
Davison A. C., Hinkley D. V., 1997, Bootstrap methods and their application. Cambridge University Press, Cambridge, UK
de Grijs R., Bono G., 2020, ApJS, 246, 3
de Grijs R., Wicker J. E., Bono G., 2014, AJ, 147, 122
Efron B., Tibshirani R., 1994, An Introduction to the Bootstrap. Chapman and Hall, London
Erler J., Ferro-Hernández R., 2020, Eur. Phys. J. C, 80, 541
Event Horizon Telescope Collaboration, 2019, ApJ, 875, L4
Farooq O., Crandall S., Ratra B., 2013, Phys. Lett. B, 726, 72
Feigelson E. D., Babu G. J., 2012, Modern Statistical Methods for Astronomy. Cambridge Univ. Press, Cambridge
Golovko V. V., 2023, Eur. Phys. J. C, 83, 930
Golovko V. V., Kamaev O., Sun J., 2023, Sensors, 23, 8856
Gott J. R., Vogeley M. S., Podariu S., Ratra B., 2001, ApJ, 549, 1
Hastie T., Tibshirani R., Friedman J., 2009, The elements of statistical learning: data mining, inference, and prediction. Springer, New York
Huber P., 1981, Robust Statistics. Wiley, New York
Ialongo C., 2019, Biochem. Med., 29, 5
James G., Witten D., Hastie T., Tibshirani R., Taylor J., 2023, An introduction to statistical learning: with applications in python. Springer Nature, New York
Kelly B. C., 2007, ApJ, 665, 1489
Kemp A. W., 2006, Steiner's Most Frequent Value. Encyclopedia of Statistical Sciences, vol. 12. John Wiley and Sons, Hoboken, New Jersey
Kim Y. J., Kang J., Lee M. G., Jang I. S., 2020, ApJ, 905, 104
Von der Linden W., Dose V., Von Toussaint U., 2014, Bayesian probability theory: applications in the physical sciences. Cambridge Univ. Press, Cambridge
Mendenhall W. M., Sincich T. L., 2016, Statistics for Engineering and the Sciences. Chapman and Hall/CRC, London
Mohan A. et al., 2024, MNRAS, 527, 10965
Penton J., Peyton J., Zahoor A., Ratra B., 2018, PASP, 130, 114001
Podariu S., Souradeep T., Gott J. R., Ratra B., Vogeley M. S., 2001, ApJ, 559, 9
Rackers N., Splawska S., Ratra B., 2024, PASP, 136, 024101
Rajan A., Desai S., 2018, Eur. Phys. J. Plus, 133, 107
Rajan A., Desai S., 2020, Prog. Theor. Exp. Phys., 2020, 013C01
Rallapalli A., Desai S., 2023, Eur. Phys. J. C, 83, 580
Ramakrishnan G., Desai S., 2023, Prog. Theor. Exp. Phys., 2023, 113F01
Rinaldi S., Middleton H., Del Pozzo W., Gair J., 2023, Eur. Phys. J. C, 83, 891
Sharma S., 2017, ARA&A, 55, 213
Singh M., Gupta S., Pandey A., Sharma S., 2016, JCAP, 8, 026
Steiner F., 1988, Geophys. Trans., 34, 139
Steiner F. (ed.), 1991, The most frequent value. Introduction to modern conception statistics. Akademia Kiado, Budapest, Hungary
Steiner F. (ed.), 1997, Optimum methods in statistics. Akademia Kiado, Budapest, Hungary
Steiner F., Hajagos B., 2001, Acta Geod. Geoph. Hung., 36, 327
Szabó N. P., Balogh G. P., Stickel J., 2018, Geophys. Prospect., 66, 530
Szegedi H., 2013, Geosci. Eng., 2, 102
Szegedi H., Dobroka M., 2014, Acta Geod. Geophys., 49, 95
Szucs P., Civan F., Virag M., 2006, Hydrogeol. J., 14, 31
Taylor J., 2022, Introduction to Error Analysis, the Study of Uncertainties in Physical Measurements, 3rd edn. Univ. Science Books, Mill Valley, CA
Wickham H., 2010, J. Comput. Graph. Stat., 19, 3
Wickham H., 2016, ggplot2: elegant graphics for data analysis. Springer, New York
Wilkinson L., 2005, The Grammar of Graphics. Springer, New York, NY
Yu H., Singal A., Peyton J., Crandall S., Ratra B., 2020, Ap&SS, 365, 146
Zahedy F. S. et al., 2021, MNRAS, 506, 877
Zhang J., 2017, MNRAS, 468, 5014
Zhang J., 2018, PASP, 130, 084502
Zhang J., Wang B., Zhang B., Han Z.-W., 2012, Chin. Phys. Lett., 29, 019701
Zhang J., Zhang S., Zhang Z.-R., Zhang P., Li W.-B., Hong Y., 2022, Eur. Phys. J. C, 82, 1106

This paper has been typeset from a TEX/LATEX file prepared by the author.